Role of Aortic Root Motion in the Pathogenesis of Aortic Dissection

Carsten J. Beller, Michel R. Labrosse, Mano J. Thubrikar and Francis Robicsek

Circulation. 2004;109:763-769
doi: 10.1161/01.CIR.0000112569.27151.F7
Circulation is published by the American Heart Association, 7272 Greenville Avenue, Dallas, TX 75231

Print ISSN: 0009-7322. Online ISSN: 1524-4539

Role of Aortic Root Motion in the Pathogenesis of Aortic Dissection

Carsten J. Beller, MD; Michel R. Labrosse, PhD; Mano J. Thubrikar, PhD; Francis Robicsek, MD, PhD

Background—The downward movement of the aortic root during the cardiac cycle may be responsible for producing the circumferential tear observed in aortic dissections.

Methods and Results—Contrast injections were investigated in 40 cardiac patients, and a finite element model of the aortic root, arch, and branches of the arch was built to assess the influence of aortic root displacement and pressure on the aortic wall stress. The axial displacement of the aortic root ranged from 0 to 14 mm. It was increased in patients with aortic insufficiency (22±13% of the sino-tubular junction diameter versus 12±9%) and reduced in patients with hypokinesis of the left ventricle (10±9% of sino-tubular junction versus 17±12%). The largest stress increase due to aortic root displacement was found approximately 2 cm above the sino-tubular junction, where the longitudinal stress increased by 50% to 0.32 Nmm^{-2} when 8.9-mm axial displacement was applied in addition to 120-mm Hg luminal pressure. A similar result was observed when the pressure load was increased to 180 mm Hg without axial displacement.

Conclusions—Both aortic root displacement and hypertension significantly increase the longitudinal stress in the ascending aorta. For patients with hypertension who are at risk of dissection, aortic root movement may be monitored as an important risk factor. **(*Circulation*. 2004;109:763-769.)**

Key Words: aorta ■ dynamics ■ stress ■ hypertension

Most aortic dissections occur with a transverse tear along the greater curvature of the aorta a few centimeters above the aortic valve.[1,2] Because mechanical stress in the aortic wall is proportional to blood pressure and vessel diameter, hypertension and aortic dilation are known risk factors for dissections. Wall abnormalities may also promote dissections,[3–5] but similar alterations have been reported in normal aging and may not alone cause dissections.[5,6]

Interestingly, these factors fail to explain the transverse orientation and the common proximal location of the tear. This is important because aortic dissection will be prevented only when its underlying causes are better identified. We propose that aortic root motion may be an additional risk factor for aortic dissection, determining both the tear location and orientation by increasing the wall stress in a specific manner.

Several studies applying cinematography and contrast injections have visualized aortic root motion wherein the root is displaced downward during systole and returns to its previous position in diastole.[7] Recent cine-MRI studies in healthy subjects revealed an axial downward motion of 8.9 mm[8] and a clockwise axial twist of 6 degrees during systole.[9]

The force driving the aortic annulus motion is the ventricular traction accompanying every heartbeat. This force is transmitted to the aortic root, the ascending aorta, the transverse aortic arch, and the supra-aortic vessels.[10] Thus, the aortic root motion has a direct influence on the deformation of the aorta and on the mechanical stress exerted on the aortic wall.

In the present study, our objective was to examine the role of the downward movement of the aortic annulus in the causation of aortic dissection. We first measured the extent of aortic root motion and then carried out a stress analysis of the aortic root, aortic arch, and supra-aortic vessels to investigate the influence of the aortic root movement on the aortic wall stress.

Methods

Measurement of Aortic Root Motion in Patients

Aortic root contrast injections on 35-mm cine films were analyzed in 40 patients (45 to 87 years old; mean age, 66 years) with coronary artery heart disease. Some patients had valvular disease, such as aortic stenosis or aortic insufficiency. Seventeen patients had undergone coronary artery bypass grafting, and 1 patient had a heart transplant. Other conditions noted were myocardial hypertrophy, left ventricular hypokinesis, and history of hypertension. No patients had aortic dissection or an obviously dilated aorta (Table 1).

Most aortograms were done in left anterior oblique projection, some in right anterior oblique view. The aortograms were projected frame by frame, and the aortic root outlines in the most upward and downward positions were traced on a transparency (Figure 1). The base of 2 sinuses and the sino-tubular junction (STJ) were marked. After digitizing the drawings, the distances between the marked points (Figure 1) were measured using Image-Pro software (Media

Received May 6, 2003; de novo received September 16, 2003; revision received November 5, 2003; accepted November 6, 2003.

From the Clinic for Cardiothoracic Surgery (C.J.B.), Heart Institute Lahr/Baden, Germany, and Heineman Medical Research Laboratory, Carolinas Medical Center, Charlotte, NC (M.R.L., M.J.T., F.R.).

Presented at the 75th Scientific Sessions of the American Heart Association, Chicago, Ill, November 17–20, 2002, and published in abstract form (*Circulation*. 2002;106[suppl II]:II-502).

Correspondence to Dr Michel R. Labrosse, Heineman Medical Research, Inc, 1000 Blythe Blvd, Charlotte, NC 28203. E-mail mrlabros@netzero.net

Circulation **is available at http://www.circulationaha.org** **DOI: 10.1161/01.CIR.0000112569.27151.F7**

TABLE 1. Measured Aortic Root Movement in Patients and Other Clinical Data

ID	Axial Displacement, % of STJ	Age, y	History of Hypertension	Ejection Fraction, %	Aortic Stenosis	Aortic Insufficiency	Hypokinesis	Hypertrophy
1	0	52	No	40			mod-sev inferior	
R2	1	70	Yes	50			mild apical	
3	1	75	No	35			mod-sev anterior	
4	2	77	No	60	mod			
R5	3	47	Yes	35			mod-sev	
R6	3	51	Yes	55		trivial		
R7	3	72	Yes	38	mild-mod			
R8	3	59	Yes	25			mod inferior	
R9	4	50	Yes	30			mod-sev	
R10	7	64	Yes	30			sev inferior	
11	7	54	Yes	60	mild	mild		
12	7	65	Yes	50				
R13	7	75	Yes	60				
14	8	51	Yes	67				
15	8	77	Yes	50		mild		
16	10	70	No		mod-sev			
17	10	58	Yes	67				
R18	11	57	No	55			mild anterior	
R19	11	71	Yes	30			mod-sev	
R20	14	75	Yes	60				
R21	14	64	Yes	67				
R22	14	62	Yes	50			mod	mod
R23	14	82	No	67		mild		
R24	15	80	No	60	mod-sev			
R25	16	64	Yes	25			mod-sev inferior	
26	17	63	No	30			mod-sev	
27	17	72	Yes	75		mild		mod
28	19	66	Yes	67				
29	20	45	Yes	20			sev inferior	
30	22	65	No			trivial		
31	22	68	Yes	60		mild		
32	23	66	Yes	65				
33	25	68	Yes	55		mild		
R34	26	87	Yes	65				
35	26	70	Yes	55	sev	trivial		mod
36	30	68	No	70	sev			
37	30	68	Yes	35	mild	mild	mod-sev anterolateral	
38	33	52	No	20				
39	37	78	Yes	75		mild		mod-sev
R40	49	82	No	15	mod	mild		

R indicates patient with previous coronary artery bypass grafting, except R21, which indicates a patient with previous heart transplant. Mod indicates moderate; sev, severe.

Cybernetics). The downward motion (axial displacement) of the aortic root, perpendicular to the plane of the STJ, was normalized by expressing it as a percentage of STJ diameter.

Statistical Analysis

The correlations between the patients' parameters and the magnitude of aortic root motion were investigated. Because the sample size was small, the analysis done was univariate. The Shapiro-Wilk test indicated the distribution of the axial displacement was not normal. Therefore, the Wilcoxon rank-sum test was used to assess the influence of aortic stenosis, aortic insufficiency, hypertrophy, hypokinesis, and hypertension on the aortic root motion. Age and ejection fraction were examined using Spearman's correlation coefficient.

Stress Analysis of the Aortic Root, Aortic Arch, and Supra-Aortic Vessels

To study the effects of aortic root motion, a finite element model of the human aortic root, aortic arch, and supra-aortic vessels was built for stress analysis using ANSYS 5.7 software (ANSYS).

Geometry

A multipronged approach was adopted to create a model representing a general, rather than patient-specific, geometry. In the model, the distance between the root base and the brachiocephalic trunk was 70 mm, and the aortic root angle to the horizontal plane in the frontal view was 30 degrees.[11] The aortic root and the ascending aorta were modeled as curved cylinders by prolongation of the arch geometry.

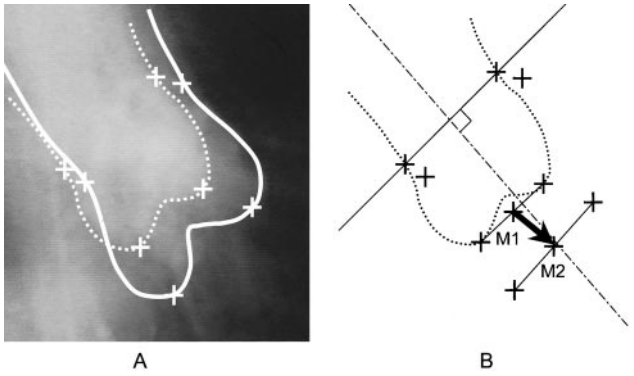

Figure 1. A, Overlaid angiograms with outlines of the most upward and downward positions of the aortic root in a cardiac cycle. †Reference points for measurement at the base of the sinuses of Valsalva and at the STJ. In schematic B, the arrow represents the movement of the base of the aortic root from M1 to M2. The projection of this displacement in the direction perpendicular to the plane of the STJ was defined as the axial displacement of the aortic root.

The actual shape of the sinuses of Valsalva was not represented because the aortic root was not the focus of the study.

The dimensions of the arch and proximal areas of the arch branches were measured previously in our laboratory from a silicone mold of a normal human aorta (S. Rao, unpublished data, 1994). The radii of the arch and the aorta were found to be 37 and 12.2 mm, respectively. The local aortic wall thickness (mean, 1.2 mm), the branches radii, and the local curvature radius and thickness at the bifurcations were implemented as determined by Rao.

To determine the arch spatial orientation, a 3D MRI reconstruction of the aortic arch and supra-aortic vessels was obtained at our center in a healthy volunteer. We found the aortic arch to lie approximately in a vertical plane oriented 20 degrees anteroposteriorly. The 3D reconstruction also established the geometry of the aortic arch branches.

Finite Elements

The model was discretized into 14 707 brick elements (Figure 2). The material properties of the aortic wall were represented as homogeneous, incompressible, linear elastic, and isotropic, with a Young's modulus of 3 Nmm^{-2} (1 Nmm^{-2}=1000 kPa=7500 mm Hg) and a Poisson's ratio of 0.49. For the aorta to deform in a physiological way, the distal ends of the supra-aortic vessels and the aorta were fixed in all directions, and stiffer material properties (Young's modulus of 12 Nmm^{-2}) were used to increase the influence of the tethering at the distal ends of the aortic arch branches.

Loading

A luminal pressure of 120 mm Hg was the only load in the control model. Then, additionally, 8.9-mm axial displacement and 6-degree twist were applied to the aortic root base. Figure 2 shows the undeformed structure and the deformed shape outline under the combined loading conditions.

To compare the effect of root motion versus hypertension on the stress in the aortic wall, the analysis was also carried out for a luminal pressure of 180 mm Hg. Other loading conditions were implemented to investigate how increased axial displacement (15 mm), twist (14 degrees), and aortic wall stiffness (Young's modulus of 6 Nmm^{-2}) may influence the aortic wall stress. Fourteen-degree twist was reported in patients with aortic stenosis.[9]

Results

Magnitude of Aortic Root Motion in Patients

The downward axial displacement of the aortic root during the cardiac cycle ranged between 0% and 49% of the STJ diameter (Table 1), with a mean of 15±11%. In most patients, the normalized axial displacement was between 0% and 20% (Figure 3).

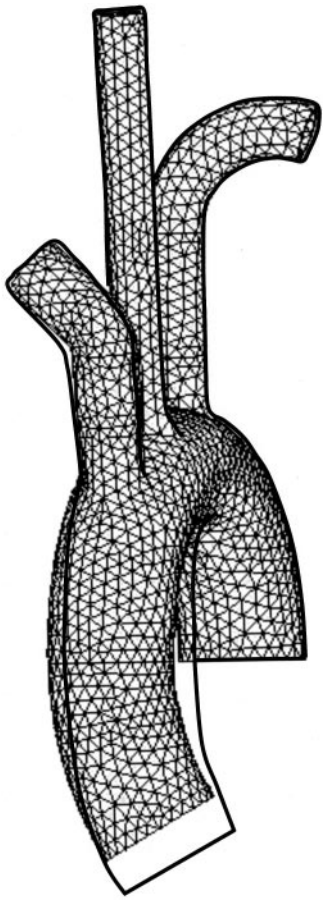

Figure 2. Front view of the finite element model of the aortic root, arch, and branches. The undeformed mesh is shown along with the deformed shape outline when 8.9-mm axial displacement and 6-degree twist were applied to the aortic root base. One may appreciate how the model deforms in space.

Using the STJ diameter to scale the aortic root displacement was acceptable, because there were no markedly dilated aortae. To confirm this, we measured the STJ diameter and the axial displacement in a subgroup of 14 patients using the 6F (2-mm) angiocatheter diameter for distance calibration. We found the STJ diameters to be normal (25±4 mm) and the aortic root displacements to range between 1 and 14 mm.

Effect of Cardiac Pathology on Aortic Root Movement

Because patients with AI have increased stroke volume, they were expected to experience increased aortic root motion. Indeed, their root movement was found to be 22±13% of STJ, as opposed to 12±9% in patients without AI (P=0.021).

Patients with left ventricular hypokinesis have reduced ventricular traction and therefore were expected to show reduced aortic root motion. Their root movement was significantly reduced to 10±9% of STJ, versus 17±12% in patients without hypokinesis (P=0.042).

The effect of myocardial hypertrophy was uncertain, and it only showed a trend to increase the aortic root movement

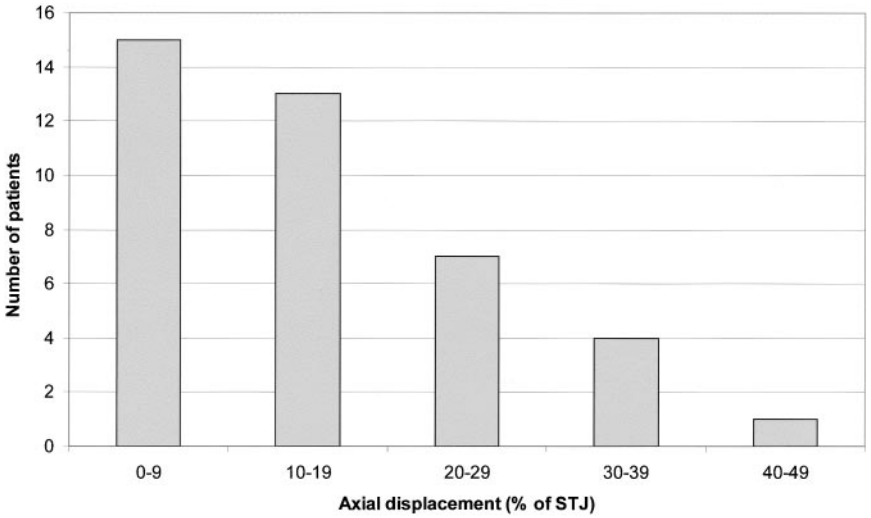

Figure 3. Frequency histogram of axial aortic root displacement expressed as a percentage of the STJ diameter and grouped by decades in 40 cardiac patients.

compared with patients without hypertrophy (24±10% of STJ versus 14±11%, $P=0.078$). The fibrotic adhesions due to previous cardiac operations may have been responsible for reducing aortic root motion to 12±11% of STJ, compared with 17±11% in patients without previous operations ($P=0.094$).

The axial root displacement was not correlated to patients' age or ejection fraction. A history of hypertension or aortic stenosis did not influence the aortic root motion.

Stress Analysis

Below we describe how the model deformed and how blood pressure, aortic root motion, and aortic wall stiffness influenced the stress exerted on the aortic wall.

Deformed Shape

Pressurization alone did not appreciably deform the model, but adding 8.9-mm axial displacement and 6-degree twist at the root base caused significant deformation, especially in the ascending aorta and the brachiocephalic trunk (Figure 2). In the vertically downward direction, this loading resulted in displacements of 7.5 mm at the root base and approximately 3 mm at the brachiocephalic trunk origin (Figure 4). In the direction perpendicular to the plane of the transverse arch, the loading induced displacements of 4 mm at the root base and approximately 2 mm at the brachiocephalic trunk level (Figure 4).

Stresses With Pressure Load, Without Aortic Root Motion

Figure 5 shows the results for mechanical stress in the control model subjected to 120-mm Hg pressure. The stresses are averaged across the vessel wall thickness and displayed in the toroidal coordinate system attached to the aortic arch. Therefore, the specification of local orientation is only valid in the region of interest including the aortic arch and the ascending aorta. As expected, stress concentrations were present at the ostia of the supra-aortic vessels. Between the brachiocephalic trunk and the left common carotid artery (LCCA), the circumferential stress was approximately 0.40 Nmm^{-2} and the longitudinal stress was approximately 0.25 Nmm^{-2}. Above the STJ, the circumferential and longitudinal stresses in the aortic wall were 0.32 and 0.21 Nmm^{-2}, respectively (Table 2).

At a pressure of 180 mm Hg, the stress between the origin of the brachiocephalic trunk and the LCCA was approximately 0.68 Nmm^{-2} in the circumferential direction and approximately 0.27 Nmm^{-2} in the longitudinal direction. Above the STJ, the circumferential and longitudinal stresses were 0.49 and 0.34 Nmm^{-2}, respectively (Table 2).

Stresses With Pressure Load and Aortic Root Motion

At 120-mm Hg luminal pressure, the circumferential and longitudinal stresses did not change markedly between the brachiocephalic trunk and the LCCA when aortic root motion was applied. The area where the most significant changes occurred was approximately 2 cm above the STJ; whereas the circumferential stress was unchanged, the longitudinal stress increased by 50%, up to 0.32 Nmm^{-2} with 8.9-mm axial displacement (Figure 6). At the highest value of axial dis-

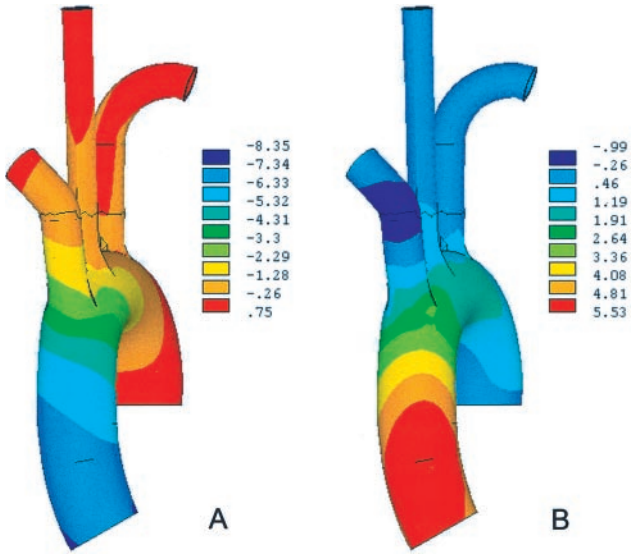

Figure 4. Displacement (mm) vertically downward (A) and perpendicular to the plane of the arch (B). In this model, the luminal pressure was 120 mm Hg, the axial displacement was 8.9 mm, and the twist at the base was 6 degrees.

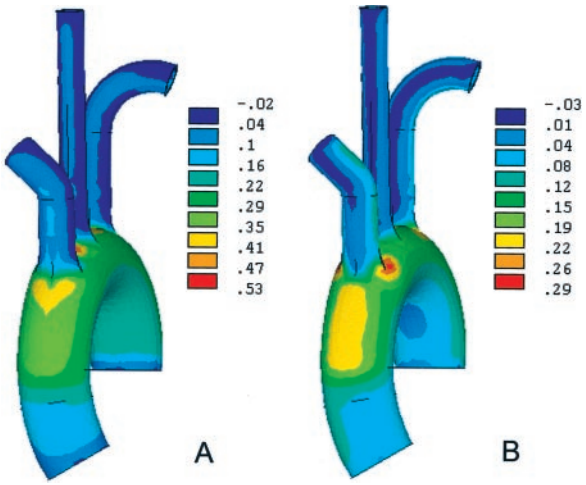

Figure 5. Distribution of circumferential (A) and longitudinal (B) stresses (Nmm^{-2}) in the aortic arch (see text). In this control model, the only load was 120-mm Hg luminal pressure. Expected stress concentrations around the ostia of the supra-aortic vessels were observed.

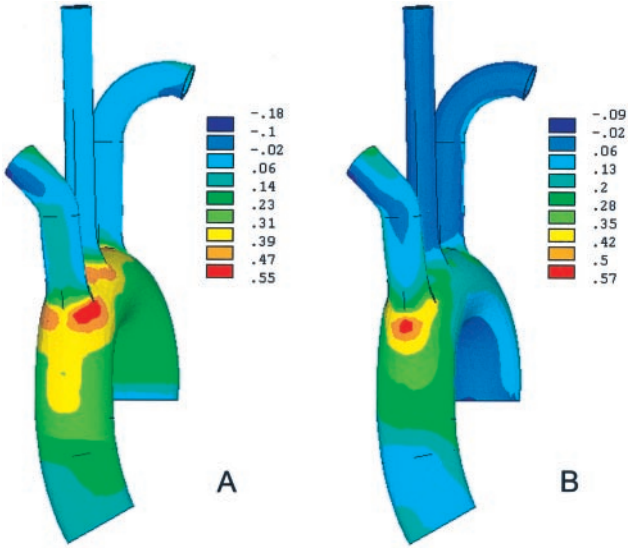

Figure 6. Same as Figure 5, with 8.9-mm axial displacement and 6-degree twist applied to the aortic root base in addition to the 120-mm Hg pressure. In this model, the longitudinal stress in the ascending aorta rose by approximately 50% compared with the control model.

placement (15 mm), the longitudinal stress was additionally increased to 0.47 Nmm^{-2}. It ultimately reached 0.64 Nmm^{-2} when the stiffness of the aorta was doubled to simulate the rigidity one may encounter in older subjects (Table 2).

Similar findings were observed with a pressure of 180 mm Hg. Adding 8.9-mm axial displacement increased the longitudinal stress above the STJ from 0.34 Nmm^{-2} to 0.41 Nmm^{-2}. It rose additionally to 0.56 Nmm^{-2} with 15-mm axial displacement or to 0.57 Nmm^{-2} when the stiffness of the aorta was doubled without increasing the displacement (Table 2).

With 15-mm axial displacement and 120-mm Hg luminal pressure, the longitudinal stress in the ascending aorta was even higher than with 8.9-mm displacement and 180-mm Hg pressure (Table 2).

Aortic Wall Stiffness

Stiffening the aorta to simulate aging did not markedly increase the stresses in the aortic wall, except when aortic root motion was introduced, which increased the longitudinal stress in the ascending aorta (Table 2).

Twist

The twist was not found to appreciably influence the deformation of the aorta, nor did it significantly alter the circumferential and longitudinal stresses (Table 2), even when the value of 14 degrees was implemented.

Discussion

Magnitude of Aortic Root Motion in Patients

Our measurements of the aortic annulus axial displacement from 2D angiograms (0 to 14 mm; 0% to 49% of STJ) were comparable with published 3D MRI measurements, ie, 6.4 to 11.3 mm in healthy subjects and 3.4 to 10.2 mm in patients with aortic regurgitation.[8] Relative measurements in terms of

TABLE 2. Wall Stress in the Ascending Aorta Approximately 2 cm Above the Sinotubular Junction

Pressure, mm Hg	Axial Displacement, mm	Twist, degree	Circumferential Stress, Nmm^{-2}	Longitudinal Stress, Nmm^{-2}
120	0	0	0.32±0.03	0.21±0.02
120	8.9	0	0.34±0.05	0.32±0.04
120	8.9	6	0.35±0.04	0.32±0.04
120	8.9	14	0.34±0.04	0.31±0.04
120	15	0	0.31±0.06	0.47±0.06
Stiff 120	15	0	0.33±0.08	0.64±0.10
180	0	0	0.49±0.05	0.34±0.03
180	8.9	0	0.47±0.06	0.41±0.05
180	15	0	0.47±0.07	0.56±0.07
Stiff 180	8.9	0	0.42±0.06	0.57±0.07

In Stiff models, the elastic modulus of the aorta was 6 Nmm^{-2} instead of the 3 Nmm^{-2} in the other models.

the STJ diameter were convenient and proved reliable provided that the diameter was kept in a normal range.

Effect of Cardiac Pathology on Aortic Root Movement

As expected, aortic insufficiency enhanced root motion, parallel to increasing stroke volume. In contrast, aortic root motion was reduced in cases of left ventricular hypokinesis, probably because of decreased ventricular traction. Multivariate studies in larger numbers of patients would be helpful to confirm these findings and examine the potential effects of other conditions, such as myocardial hypertrophy and previous coronary artery bypass grafting.

Applicability of the Model

To our knowledge, this is the first model examining aortic root motion, hypertension, and wall stiffness as factors modifying the wall stress in different areas of the aorta. Although the mold prepared for arch measurements was cast at 40-mm Hg pressure, the resulting geometry was considered valid at systemic pressure, for its thickness-to-radius ratio was close to 1:8, as seen in vivo.[12] Tissue anisotropy and residual stress were not addressed. The results were not markedly dependent on the mesh size. Indeed, doubling the element number to 30 951 changed the average stresses in the ascending aorta by at most 6.3%. The material model for the vessels was linear elastic for stress analysis with regard to the geometry at 80 mm Hg, ie, in the high modulus region.[13] The specific stress values found may be affected by the simplified material properties, but it is believed that the overall findings of the study are not.

The geometry of the model was comparable with a 3D MRI reconstruction and included the details of the ostia of the aortic arch vessels and changes in aortic wall thickness of a human sample. When the aortic root motion was enforced as described in the literature,[8,9] proper tethering of the model made it possible to reproduce published data on the displacements perpendicular to the plane of the transverse aorta, ie, 3.5 mm at the aortic root level and 2.2 mm in the transverse region,[14] whereas the computed results were 4 mm and approximately 2 mm, respectively. The 3-mm downward pull at the brachiocephalic trunk origin also matched qualitative data gathered from cine-MRI.

Significance of Aortic Wall Stress

Like other arterial bifurcations,[15–17] the ostia of the aortic arch branches are areas of stress concentration, but they exhibit reinforced vascular architecture and are not typical locations of dissections.[1] In contrast, we showed that the right lateral aspect of the ascending aorta a few centimeters above the STJ experienced increased longitudinal stress with increased axial displacement, pressure, and aortic wall stiffness. This area may be at risk of tissue degeneration and intimal rupture. It is also where the band-like thickening of the pericardium is suspected of reducing the aortic mobility and enhancing wall stress.[1]

A yield stress of 1.2 Nmm^{-2} was reported for the abdominal aortic wall in the longitudinal direction.[18] This may be a conservative estimate for the yield stress of the thoracic aorta, also known for having a lower breaking strength longitudinally than transversely.[19] In our model, the longitudinal stress reached only approximately half this value, but the probable weakness of the intimal layer was not considered. Regardless, as the ratio of longitudinal to circumferential stress increases, there may be an increased risk for a circumferential tear to develop, as observed in most aortic dissections.[1] Note that only average transmural stresses were reported here, because their gradient cannot be determined using the homogeneous wall hypothesis.

The postulate that aortic root motion and, ultimately, the force applied by the left ventricle play an important role in the development of dissections is supported by important clinical observations. Beavan and Murphy[20] found a dramatic increase in the aortic dissection rates among hypertensive patients treated with hexamethonium. This was attributed to the inotropic effect of hexamethonium on cardiac contractions. Considering our findings, hexamethonium may have increased aortic root motion and caused a higher incidence of dissections. Also, turkeys, known for their high blood pressure (up to 400 mm Hg), are prone to aortic rupture. In susceptible flocks, aortic ruptures can be prevented by administration of reserpine in a dosage with little effect on the blood pressure but effectively depleting cardiac catecholamines and reducing cardiac contractility.[21]

It is important to state that root motion alone is only an indicator of the force that the heart exerts on the aorta. Thus, a large aortic root displacement may be well tolerated in a compliant aorta or may cause a disaster in a subject with stiffer aortic tissue.

Other Clinical Implications of Aortic Root Motion

As an aortic aneurysm dilates, the longitudinal stress in the bulb rises significantly and may cause rupture.[22] By additionally increasing the longitudinal stress, aortic root motion may enhance the chances of rupture of small aneurysms not considered for surgical intervention. Aortic root motion may also dislodge atherosclerotic debris from the aortic wall and cause strokes or other embolic events[23] or lead to accelerated degeneration of homografts, autografts, and bioprosthetic valves.

Conclusions

The aortic root motion has a direct impact on the mechanical stresses acting on the aorta. The longitudinal stress was found to increase critically in the ascending aorta above the STJ. This may explain why circumferential intimal tears and aortic dissections occur more often in this location. Functional downward displacement of the aortic root seemed to be as much of a risk factor for dissection as hypertension. Increased stiffness was also found to enhance the effects of root motion on aortic wall stress. For all the above reasons, in patients possibly at risk of dissection, aortic root movement should be considered an additional risk factor.

References

1. Hirst AE, Johns VJ, Kime SW. Dissecting aneurysms of the aorta: a review of 505 cases. *Medicine (Baltimore)*. 1958;37:217–279.
2. Edwards JE. Manifestations of acquired and congenital diseases of the aorta. *Curr Probl Cardiol.* 1979;3:1.

3. Sabiston DC Jr, Spencer FC. *Surgery of the Chest, Volume II*. 5th ed. Philadelphia: WB Saunders; 1990:1201.
4. Doroghazi RM, Slater EE. *Aortic Dissection*. New York: McGraw-Hill; 1983:38.
5. Leonard JC, Hasleton PS. Dissecting aortic aneurysms: a clinicopathological study. *Q J Med*. 1979;XLVIII:55–76.
6. Schlatmann TJM, Becker AE. Pathogenesis of dissecting aneurysm of aorta: comparative histopathologic study of significance of medial changes. *Am J Cardiol*. 1977;39:21–26.
7. Mercer JL. Movement of the aortic annulus. *Br J Radiol*. 1969;42: 623–626.
8. Kozerke S, Scheidegger MB, Pedersen EM, et al. Heart motion adapted cine phase-contrast flow measurements through the aortic valve. *Magn Reson Med*. 1999;42:970–978.
9. Stuber M, Scheidegger MB, Fischer SE, et al. Alterations in the local myocardial motion pattern in patients suffering from pressure overload due to aortic stenosis. *Circulation*. 1999;100:361–368.
10. Wheat MW Jr. Pathogenesis of aortic dissection. In: Doroghazi RM, Slater EE, eds. *Aortic Dissection*. New York: McGraw-Hill; 1983: 55–60.
11. Liotta D, Del Rio M, Cooley DA, et al. *Diseases of the Aorta*. Argentina: Domingo Liotta Foundation Medical; 2001:1–22.
12. Nichols WW, O'Rourke MF. *McDonald's Blood Flow in Arteries: Theoretical, Experimental and Clinical Principles*. 4th ed. London: Edward Arnold; 1998.
13. Holzapfel GA, Gasser TC, Ogden RW. A new constitutive framework for arterial wall mechanics and a comparative study of material models. *J Elasticity*. 2000;61:1–48.
14. Duvernoy O, Coulden R, Ytterberg C. Aortic motion: a potential pitfall in CT imaging of dissection in the ascending aorta. *J Comput Assist Tomogr*. 1995;19:569–572.
15. Salzar RS, Thubrikar MJ, Eppink RT. Pressure-induced mechanical stress in the carotid artery bifurcation: a possible correlation to atherosclerosis. *J Biomech*. 1995;28:1333–1340.
16. Delfino A, Stergiopoulos N, Moore JE, et al. Residual strain effects on the stress field in a thick wall finite element model of the human carotid bifurcation. *J Biomech*. 1997;30:777–786.
17. Thubrikar MJ, Roskelley SK, Eppink RT. Study of stress concentration in the walls of the bovine coronary arterial branch. *J Biomech*. 1996;23: 15–26.
18. Raghavan ML, Webster MW, Vorp DA. Ex-vivo biomechanical behavior of abdominal aortic aneurysm: assessment using a new mathematical model. *Ann Biomed Eng*. 1996;24:573–582.
19. Mohan D, Melvin JW. Failure properties of passive human aortic tissue, II: biaxial tension test. *J Biomech*. 1983;16:31–44.
20. Beaven DW, Murphy EA. Dissecting aneurysm during methonium therapy: a report on nine cases treated for hypertension. *Br Med J*. 1956;Jan 14:77–80.
21. Carlson CW. Further studies with reserpine for growing turkeys and laying hens. In: *Second Conference on Use of Reserpine in Poultry Production*. St Paul, Minn: 1960;25.
22. Thubrikar MJ, Agali P, Robicsek F. Wall stress as a possible mechanism for the development of transverse intimal tears in aortic dissections. *J Med Eng Technol*. 1999;23:127–134.
23. Fayar ZA, Nahar T, Fallon JT, et al. In vivo magnetic resonance evaluation of atherosclerotic plaques in the human thoracic aorta: a comparison with transesophageal echocardiography. *Circulation*. 2000;101: 2503–2509.